Proteomics
Clinical Applications
www.clinical.proteomics-journal.com

MALDI-IMS as a Tool to Determine the Myocardial Response to Syndecan-2-Selected Mesenchymal Stromal Cell Application in an Experimental Model of Diabetic Cardiomyopathy

Kathleen Pappritz, Oliver Klein, Fengquan Dong, Nazha Hamdani, Arpad Kovacs, Lisa O'Flynn, Steve Elliman, Timothy O'Brien, Carsten Tschöpe, and Sophie Van Linthout**

Purpose: Mesenchymal stromal cells (MSC) are an attractive tool for treatment of diabetic cardiomyopathy. Syndecan-2/CD362 has been identified as a functional marker for MSC isolation. Imaging mass spectrometry (IMS) allows for the characterization of therapeutic responses in the left ventricle. This study aims to investigate whether IMS can assess the therapeutic effect of $CD362^+$-selected MSC on early onset experimental diabetic cardiomyopathy.

Experimental Design: 1×10^6 wild type (WT), $CD362^-$, or $CD362^+$ MSC are intravenously injected into db/db mice. Four weeks later, mice are hemodynamically characterized and subsequently sacrificed for IMS combined with bottom-up mass spectrometry, and isoform and phosphorylation analyses of cardiac titin.

Results: Overall alterations of the cardiac proteome signatures, especially titin, are observed in db/db compared to control mice. Interestingly, only $CD362^+$ MSC can overcome the reduced titin intensity distribution and shifts the isoform ratio toward the more compliant N2BA form. In contrast, WT and $CD362^-$ MSCs improve all-titin phosphorylation and protein kinase G activity, which is reflected in an improvement in diastolic performance.

Conclusions and Clinical Relevance: IMS enables the characterization of differences in titin intensity distribution following MSC application. However, further analysis of titin phosphorylation is needed to allow for the assessment of the therapeutic efficacy of MSC.

1. Introduction

Diabetes mellitus is a global epidemic that is expected to affect over 600 million people worldwide by 2045.[1] Despite enormous advances in therapy options and patient self-management, diabetes represents a growing medical and economic problem. Cardiovascular events, including diabetic cardiomyopathy, are the leading cause of morbidity and mortality in diabetic patients. Diabetic cardiomyopathy, first discovered by Rubler et al. in 1972,[2] describes structural and functional alterations of the heart, which are independent of coronary artery disease and hypertension. Hallmarks of diabetic cardiomyopathy are interstitial inflammation[3] and fibrosis,[4] impaired vascularization, and cardiomyocyte stiffness.[5] Left ventricular (LV) diastolic dysfunction, attributed to excessive collagen deposition,[6] and cardiomyocyte stiffness,[7] represents the earliest preclinical manifestation of diabetic cardiomyopathy.[8]

The molecular alterations in the myocardium due to diabetic cardiomyopathy

Dr. K. Pappritz, Dr. O. Klein, Dr. F. Dong, Prof. C. Tschöpe, Dr. S. Van Linthout
Berlin-Brandenburg Center for Regenerative Therapies and Berlin Institute of Health Center for Regenerative Therapies (BCRT)
Charité – Universitätsmedizin Berlin
Campus Virchow Klinikum (CVK), Berlin 13353 and 10178, Germany
E-mail: kathleen.pappritz@charite.de; sophie.van-linthout@charite.de

The ORCID identification number(s) for the author(s) of this article can be found under https://doi.org/10.1002/prca.202000050

DOI: 10.1002/prca.202000050

Dr. K. Pappritz, Dr. O. Klein, Prof. C. Tschöpe, Dr. S. Van Linthout
German Center for Cardiovascular Research (DZHK)
Partner site Berlin
Berlin 13347, Germany

Dr. N. Hamdani, Dr. A. Kovacs
Department of Physiology
Institute of Physiology
Ruhr University Bochum
Bochum 44780, Germany

Dr. L. O'Flynn, Dr. S. Elliman
Orbsen Therapeutics
National University of Ireland (NUIG)
Galway H91 TK33, Ireland

Prof. T. O'Brien
Regenerative Medicine Institute and Department of Medicine
NUIG
Galway H91 TK33, Ireland

remain poorly understood despite extensive research in the field. This is largely owing to the heterogeneity of cardiac tissue. Traditional histological stainings that are currently used can only provide limited information about the tissue, depending on the specific staining used. To overcome these limitations, label-free and multiplex in situ analysis techniques are attracting increasing interest. Matrix-assisted laser desorption/ionization imaging mass spectrometry (MALDI-IMS) is a promising label-free multiplex technology that enables precision tissue assessment based on label-free in situ spatially resolved molecular signatures (e.g., metabolites, peptides, and proteins). This allows for correlation of the detected signature with alterations in tissue histology.[9,10]

Our own previous data on streptozotocin (STZ)-induced type 1 diabetes mellitus-associated diabetic cardiomyopathy demonstrated that MALDI-IMS, in combination with speckle-tracking echocardiography, is able to assess region-dependent alterations in protein distribution and the associated impairment of global and regional LV deformation.[11] Along with the differentiation and classification of pathophysiological regions,[12] studies in patients revealed the capability of IMS to stratify patients[13] and to characterize the therapeutic response.[14,15]

Recent studies on early stage diabetic cardiomyopathy showed that dysfunctionality of the contractile apparatus,[16] including myosin and titin,[5,17] is sufficient to induce diastolic dysfunction without any involvement of cardiac fibrosis. Given their ability to reduce cardiomyocyte stiffness,[5] MSC are an attractive tool for the treatment of diabetic cardiomyopathy. Syndecan-2/CD362, a heparin sulfate proteoglycan, is expressed on the surface of a subpopulation of human MSC, allowing the selective isolation of a homogenous cell population, which meets regulatory requirements for clinical use. Masterson et al.[18] recently demonstrated that human CD362$^+$ MSC decreased *Escherichia coli*-induced pneumonia severity and that their efficacy was at least comparable to heterogeneous human MSCs. However, the potential of CD362$^+$ MSC in improving experimental diabetic cardiomyopathy has not been investigated before.

Therefore, the aim of the present proof-of-concept study was to evaluate whether IMS can assess the therapeutic effect of CD362$^+$-selected MSC in early onset experimental diabetic cardiomyopathy.

Clinical Relevance

Diabetes mellitus represents a growing medical and economic problem. A common complication of diabetes mellitus is diabetic cardiomyopathy, a specific cardiac disorder associated with cardiac dysfunction and cardiac structural alterations. Mesenchymal stromal cells (MSC) are an attractive cell-type for cardiac cell therapy. In the context of a clinical therapeutic cell product, a clearly defined population of MSC is required, which is possible using syndecan-2/CD362 selection. This study aimed to assess the therapeutic effect of wild type (WT), CD362$^-$, and CD362$^+$ MSC application in db/db mice, a model of diabetic cardiomyopathy, using imaging mass spectrometry (IMS). IMS was able to identify decreased intensity distribution of cardiac titin in db/db mice, which was normalized after CD362$^+$ MSC administration. In contrast, titin phosphorylation was only increased after WT or CD362$^-$ MSC application, accompanied by restored protein kinase G (PKG) activity and improved diastolic function in db/db mice. Our study highlights the strength of IMS to assess local changes in protein distribution in myocardial tissue in response to MSC. However, it also points out that to enable molecular assessment of the therapeutic efficacy of MSC during early onset diabetic cardiomyopathy, evaluation of the phosphorylation state of titin is needed.

2. Results

2.1. Intravenously Applied Syndecan-2-Selected Mesenchymal Stromal Cells Induce Subtle Alterations of the Cardiac Proteome in Type 2 Diabetic db/db Mice

For all experimental groups, primary proteomic screening via MALDI-IMS was performed (Table S1, Supporting Information). In total, 298 m/z values ranging from 802.113 to 3198.652 Da were detected. Peptide signatures in the different groups are illustrated by average mass spectra in **Figure 1**A. In order to determine the largest differences between the groups, principal component analysis (PCA) was performed, in which differences between LV tissue of non-diabetic db+/db versus diabetic db/db mice were captured (PC-1 = 31.69%; Figure 1B, left panel). Administration of WT, CD362$^-$ and CD362$^+$ MSC in db/db mice resulted in no differences compared to the db+/db mice (PC-1 28.88–31.66%; Figure 1B, mid-left panel until right panel).

2.2. Intravenously Applied Syndecan-2-Selected Mesenchymal Stromal Cells Change the Signature of 18 Proteins in Type 2 Diabetic db/db Mice

In order to get further insights into which proteins were changed due to MSC application, m/z values were subsequently identified via bottom-up liquid chromatography-based mass spectrometry (LC-MS; Table S2, Supporting Information). The individual protein signatures from each group were compared in a pairwise manner to obtain discriminative peptide values by using ROC analysis. ROC analysis resulted in 76 peptide values that distinguished db+/db and db/db mice, 58 that distinguished db/db and db/db WT mice, 101 that distinguished between db/db and db/db CD362$^-$ mice, and 51 that discriminated between db/db and db/db CD362$^+$ mice (AUC > 0.6 or < 0.4; $p < 0.01$; Table S1, Supporting Information). Subsequently, discriminative m/z values from IMS were assigned to a LC-MS reference list (Table S2, Supporting Information) for protein identification.[19]

Prof. C. Tschöpe
Department of Cardiology
Charité – Universitätsmedizin Berlin
CVK Berlin 13353, Germany

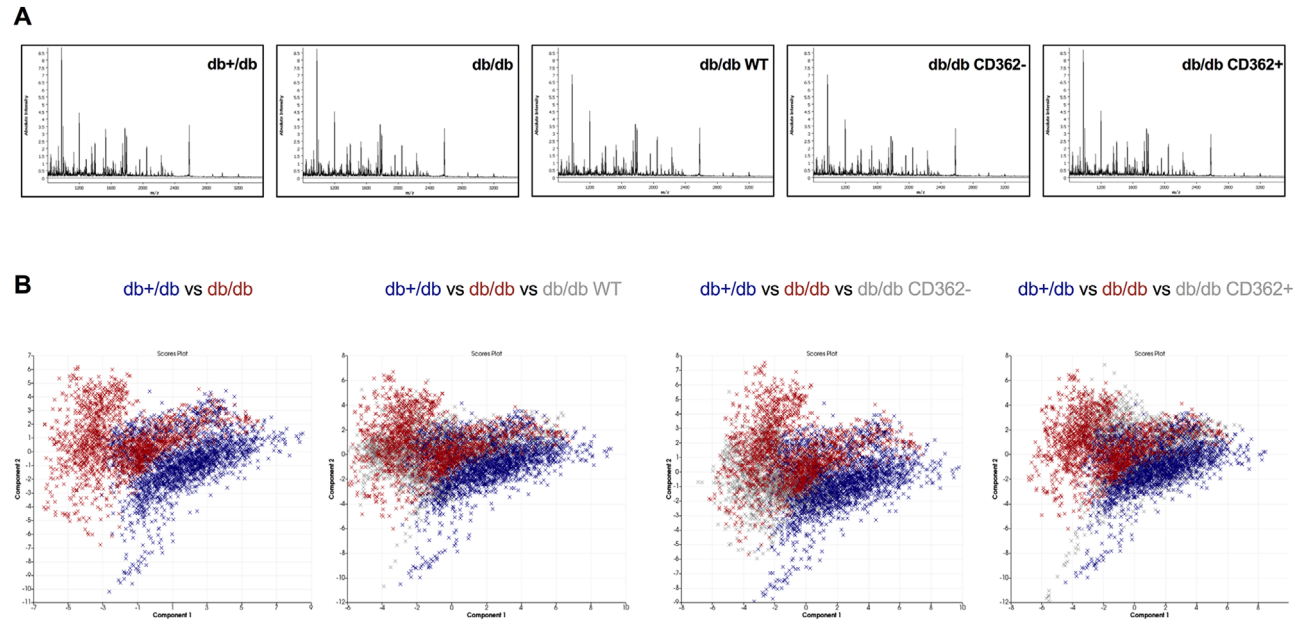

Figure 1. Intravenously applied syndecan-2-selected mesenchymal stromal cells induce subtle alterations of the cardiac proteome in type 2 diabetic db/db mice. A) Average peptide spectra of left ventricular (LV) tissue derived from db+/db, db/db, db/db WT, db/db CD362$^-$, and db/db CD362$^+$ mice. B) PCA showed differences in the cardiac proteome of the db+/db (blue spots) versus db/db group (red spots; left panel). Application of the different MSC types (gray spots) induced minimal changes in the cardiac protein composition.

In accordance to our criteria that more than one peptide is required for protein identification, a list of 77 m/z values from the initial 298 m/z values were assigned to 18 proteins and could be assumed as correctly identified according to the guidelines[19] (Table S3, Supporting Information).

2.3. Intravenously Applied Syndecan-2-Selected Mesenchymal Stromal Cells Alter the Intensity Distribution of Cardiac α-actin, ATP Synthase, Myosin-6/7, and Titin in Type 2 Diabetic db/db Mice

To further determine the therapeutic impact of MSC application in type 2 db/db mice, ROC analysis of the 18 proteins was performed. Only isoforms with two similar discriminate characteristics and an AUC >0.6 or <0.4 for the different comparisons were assumed as correctly identified. As a result, α-actin cardiac muscle 1 (Actc1), ATP synthase subunit α, mitochondrial (Atp5a1), glyceraldehyde-3-phosphate dehydrogenase (Gapdh), myosin-6/7 (Myh6/Myh7), and titin (Ttn) were assigned to the observed m/z values from the MALDI-IMS experiment (**Table 1**).

Illustration of spatial intensity distribution indicated a higher expression of cardiac α-actin (**Figure 2**A) and mitochondrial ATP synthase (Figure 2B) in db/db versus db+/db mice. Interestingly, application of CD362$^-$ and CD362$^+$ MSC in db/db mice lowered the intensity distribution of both proteins compared to untreated db/db mice, whereas WT MSC only reduced the intensity distribution of mitochondrial ATP synthase. Regarding myosin-6/7, db/db animals displayed a lower intensity distribution compared to db+/db mice, which was partially restored by WT, CD362$^-$, and CD362$^+$ MSC injection (Figure 2C). In contrast, the initially lower spatial distribution of cardiac titin in db/db mice compared to controls was normalized by application of CD362$^+$ MSC, but not by WT or CD362$^-$ MSC administration to db/db mice (**Figure 3**).

2.4. Intravenously Applied Syndecan-2-Selected Mesenchymal Stromal Cells Abrogate Reduced Cardiac Titin Phosphorylation in Type 2 Diabetic db/db Mice

Titin is the largest sarcomere protein and exists in two isoforms: N2B and N2BA, whereby N2B is the shorter and stiffer form, and N2BA, the longer and more compliant form.[7] MALDI-IMS indicated significant reduction of LV titin distribution in db/db mice, which was only increased after application of CD362$^+$ MSC (Figure 3). MALDI-IMS does not allow for the distinction between the two different titin isoforms. Subsequent in depth analysis of titin isoform composition and titin phosphorylation via SYPRO Ruby and Pro-Q Diamond phosphoprotein staining on SDS gels,[5,17] revealed a lower N2BA/N2B ratio in db/db mice compared to db+/db mice (**Figure 4**A), which was accompanied by reduced titin phosphorylation in these animals (Figure 4B). Furthermore, the activity of both protein kinase G (PKG) and protein kinase A (PKA), protein kinases important in titin phosphorylation,[20] was reduced in db/db mice versus db+/db animals (Figure 4C,D).

The reduced N2BA/N2B ratio was only increased in db/db mice receiving CD362$^+$ MSC compared to db/db mice (Figure 4A). However, only WT and CD362$^-$ MSC increased titin phosphorylation and PKG activity in db/db mice (Figure 4B–D). In contrast, administration of CD362$^+$ MSC had no effect on titin phosphorylation, or on PKG activity.

Table 1. Intravenously applied syndecan-2-selected mesenchymal stromal cells alter the intensity distribution of MALDI-IMS-derived identified proteins in type 2 diabetic db/db mice. Table displayed ROC analysis of identified peptides within the different groups. As stated in the Experimental Section, peptides with lowest mass difference to the LC-MS reference list value and with similar discrimination characteristics were assumed as a match.

	ROC [AUC]									
IMS *m/z* [Da] ±0.337	db/db vs db+/db	db/db vs db/db WT	db/db vs db/db CD362$^+$	db/db vs db/db CD362$^-$	IMS-Mr [Da]	LC MS-Mr [Da]	D [Da]	Sequence	Protein	Gen
2244.087	0.61	0.41	0.44	0.57	2243.08	2243.05	0.03	K.DLYANNVLSGGTTMYPGIADR.M	Actin, alpha cardiac muscle 1	Actc1
1198.386	0.63	0.49	0.55	0.59	1197.38	1197.70	0.32	R.AVFPSIVGRPR.H		
1625.037	0.60	0.51	0.53	0.57	1624.03	1623.88	0.15	R.TGAIVDVPVGEELLGR.V	ATP synthase subunit alpha, mitochondrial	Atp5a1
1667.905	0.64	0.50	0.53	0.53	1666.90	1666.79	0.11	R.NVQAEEMVEFSSGLK.G		
1779.969	0.62	0.44	0.57	0.65	1778.96	1778.79	0.17	K.LISWYDNEYGYSNR.V	Glyceraldehyde-3-phosphate dehydrogenase	Gapdh
1032.654	0.62	0.56	0.60	0.70	1031.65	1031.59	0.06	M.VKVGVNGFGR.I		
994.512	0.28	0.45	0.32	0.59	993.50	993.51	0.01	K.TTHPHFVR.C	Myosin-6/7	Myh6/Myh7
883.461	0.32	0.51	0.38	0.53	882.45	882.46	0.01	R.ILYGDFR.Q		
1078.559	0.35	0.58	0.38	0.61	1077.55	1076.60	0.95	R.VDLIHDLPR.V	Titin	Ttn
950.631	0.37	0.55	0.47	0.62	949.62	949.52	0.10	K.ITGYIVER.R		

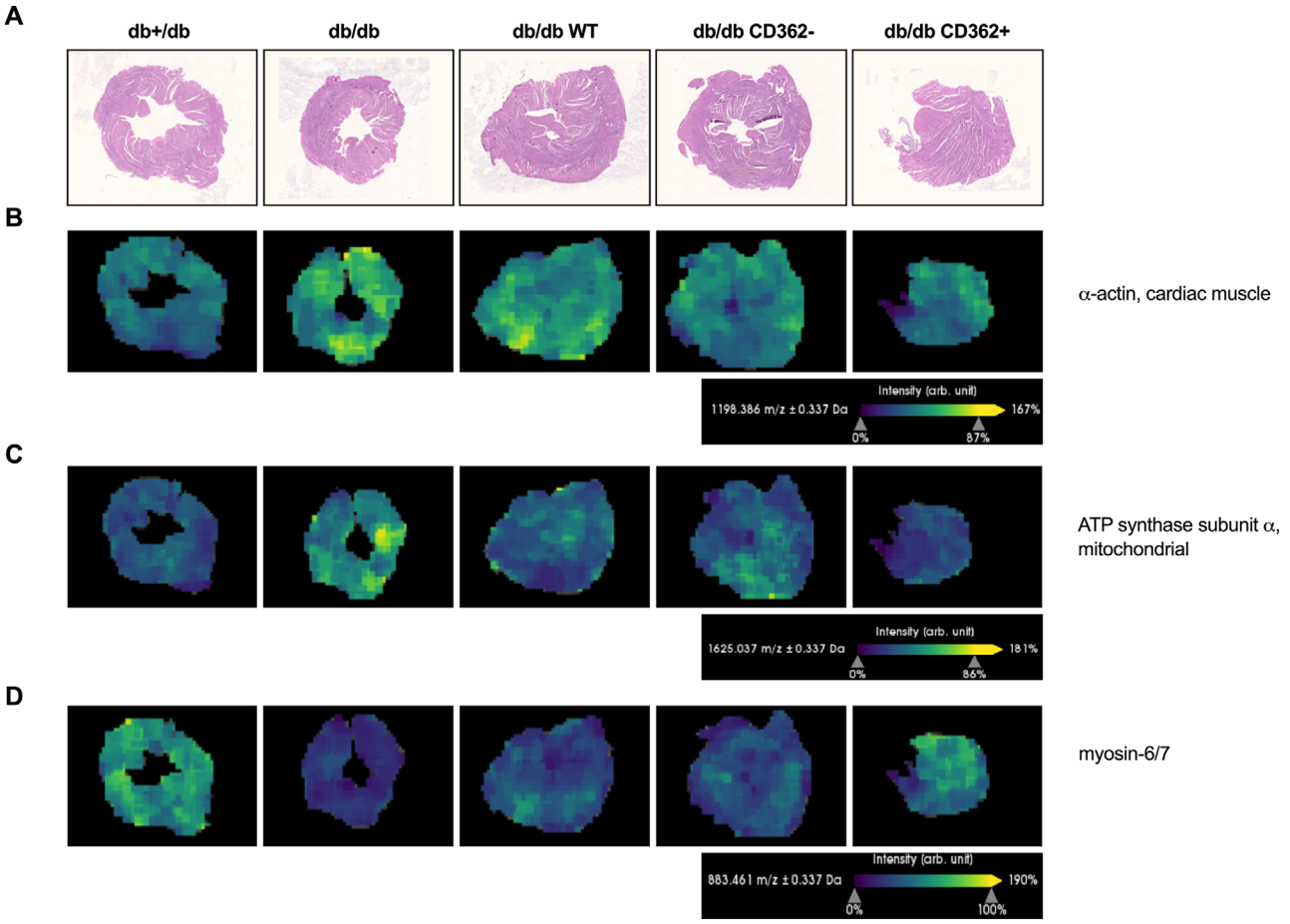

Figure 2. Intravenously applied syndecan-2-selected mesenchymal stromal cells alter intensity distribution of cardiac α-actin, ATP synthase, and myosin-6/7 in type 2 diabetic db/db mice. A) Representative H/E staining of the respective tissue slides, followed by illustration of spatial intensity distribution of B) cardiac α-actin (*m/z* 1198.386 Da), C) mitochondrial ATP synthase subunit α (*m/z* 1625.037 Da), and D) myosin-6/7 (*m/z* 883.461 Da) in LV samples of db+/db, db/db, db/db WT, db/db CD362$^-$, and db/db CD362$^+$ mice.

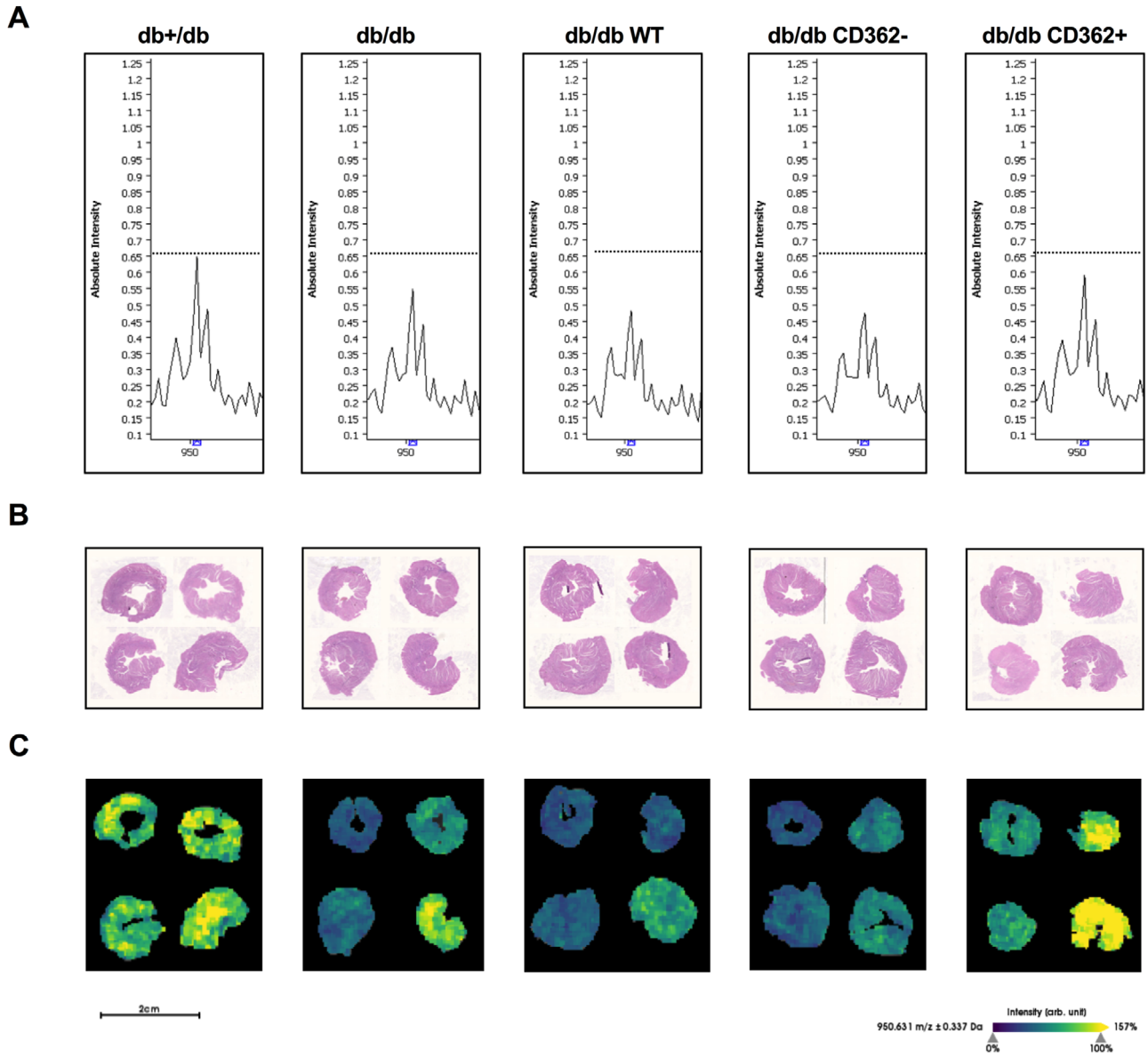

Figure 3. Intravenously applied syndecan-2-selected mesenchymal stromal cells abrogate reduced intensity distribution of cardiac titin in type 2 diabetic db/db mice. In addition to A) representative mass spectra, B) H/E staining was shown. C) The corresponding spatial intensity distribution of m/z values for all 4 LV tissue replicates indicate a lower intensity distribution of m/z 950.631 Da from cardiac titin in db/db mice versus db+/db animals. Application of WT and CD362$^-$ MSC have no impact on intensity distribution of titin, whereas CD362$^+$ cells restore titin expression.

2.5. Intravenously Applied Syndecan-2-Selected Mesenchymal Stromal Cells Do Not Ameliorate Diastolic Function in Type 2 Diabetic db/db Mice

To investigate whether the WT, CD362$^-$, and CD362$^+$ MSC-mediated effects on titin phosphorylation and PKG activity in db/db mice translated into improved contractile function, hemodynamic measurements were performed (**Figure 5**). LV contractility and relaxation parameters, dP/dt_{max} and dP/dt_{min}, respectively, were reduced in db/db mice versus db+/db animals (Figure 5A,B), accompanied by an increase in Tau (Figure 5C). Intravenous administration of WT MSC abrogated the reduced LV contractility and relaxation in db/db mice, as indicated by an increase of dP/dt_{max} and dP/dt_{min}, and decreased Tau (Figure 5A–C). Application of CD362$^-$ MSC in db/db mice also improved cardiac diastolic function compared to db/db mice, as shown by an increased dP/dt_{min} and reduced Tau (Figure 5B,C). In contrast, CD362$^+$ MSC administration improved neither LV contractility nor LV relaxation in db/db mice (Figure 5A–C).

3. Discussion

The main finding of the present study is that by using IMS we were able to characterize differences in titin intensity distribution following MSC application during early onset experimental diabetic cardiomyopathy. However, further analysis of titin

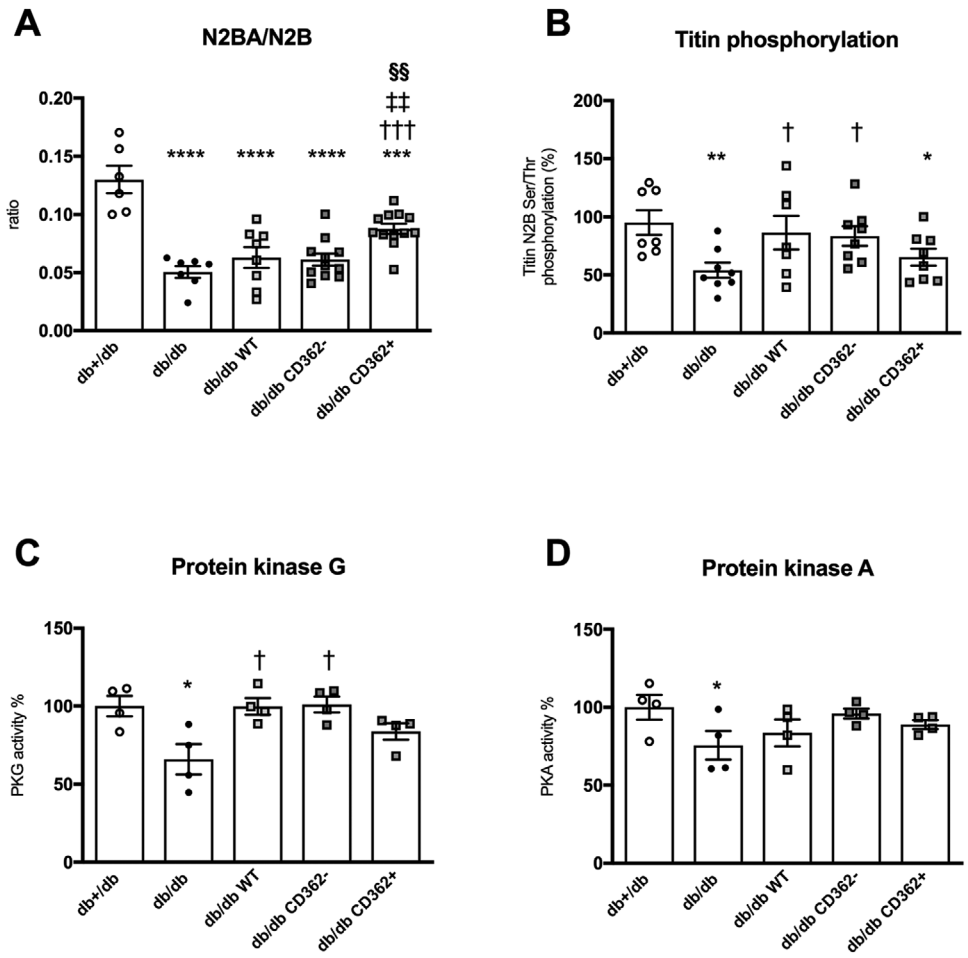

Figure 4. Intravenously applied syndecan-2-selected mesenchymal stromal cells abrogate reduced cardiac titin phosphorylation in type 2 diabetic db/db mice. A) Calculation of the N2BA/N2B ratio using Pro-Q Diamond phosphoprotein staining. B) Titin N2B Ser/Thr phosphorylation state depicted as percentage of phosphorylation toward total protein (A, B with $n = 6$ for db+/db, $n = 7$ for db/db, $n = 8$ for db/db WT, $n = 11$ for db/db CD362$^-$, and $n = 12$ for db/db CD362$^+$ group). Finally, C) PKG and D) PKA activity were measured (C, D with $n = 4$/group). Data are depicted as mean ± SEM and analyzed with one-way ANOVA or Kruskal–Wallis test (*$p < 0.05$, **$p < 0.01$, ***$p < 0.001$, ****$p < 0.0001$ vs db+/db; $^{\dagger}p < 0.05$, $^{\dagger\dagger}p < 0.01$, $^{\dagger\dagger\dagger}p < 0.001$, $^{\dagger\dagger\dagger\dagger}p < 0.0001$ vs db/db; $^{\ddagger}p < 0.05$, $^{\ddagger\ddagger}p < 0.01$, $^{\ddagger\ddagger\ddagger}p < 0.001$, $^{\ddagger\ddagger\ddagger\ddagger}p < 0.0001$ vs db/db WT; $^{\S}p < 0.05$, $^{\S\S}p < 0.01$, $^{\S\S\S}p < 0.001$, $^{\S\S\S\S}p < 0.0001$ vs db/db CD362$^-$).

phosphorylation is needed to allow the assessment of the therapeutic efficacy of MSC.

One of the common complications of diabetes mellitus is diabetic cardiomyopathy, an own clinical entity, which develops in the absence of hypertension and coronary artery disease.[2] Diabetic cardiomyopathy is associated with structural alterations of the myocardium and cardiac dysfunction.[3–6] Accumulating evidence shows that even in the absence of prominent cardiac fibrosis, diastolic LV function can be impaired due to changes in cardiac sarcomere proteins.[5,11,17] Indeed, we recently demonstrated via MALDI-IMS that STZ-induced type 1 diabetic cardiomyopathy is associated with regional-dependent changes in intensity distribution of α-actin, myosin light chain 3, and titin, which are all associated with the contractile function of the heart.[11] In the present study, we detected changes of proteins associated with contractile function (α-actin, myosin-6/7, and titin) and cardiac energy metabolism (mitochondrial ATP synthase) in db/db mice compared to db+/db animals. These data agree with previous reports investigating the cardiac proteome in experimental type 1[21] and type 2[22] diabetes mellitus, which therefore highlights the particular relevance of these signaling pathways in the pathogenesis of diabetic cardiomyopathy.[23]

MSC are an attractive tool to treat diabetic cardiomyopathy given their well-established immunomodulatory, endothelial-protective, and anti-fibrotic features and their ability to improve diastolic function via their impact on titin regulation.[5] Furthermore, application of WT and CD362$^-$ MSC in db/db mice, a well-accepted experimental model to study type 2 diabetes mellitus,[24] results in an improvement of diastolic function. Interestingly, application of the different MSC types resulted in only subtle changes of the total cardiac proteome. Further protein identification and ROC analyses revealed decreased myosin-6/7 and titin intensity distribution in diabetic db/db mice, which was partially improved after CD362$^+$ MSC administration. Similar observations were made in STZ mice treated with placenta-derived adherent stromal cells[5] and in

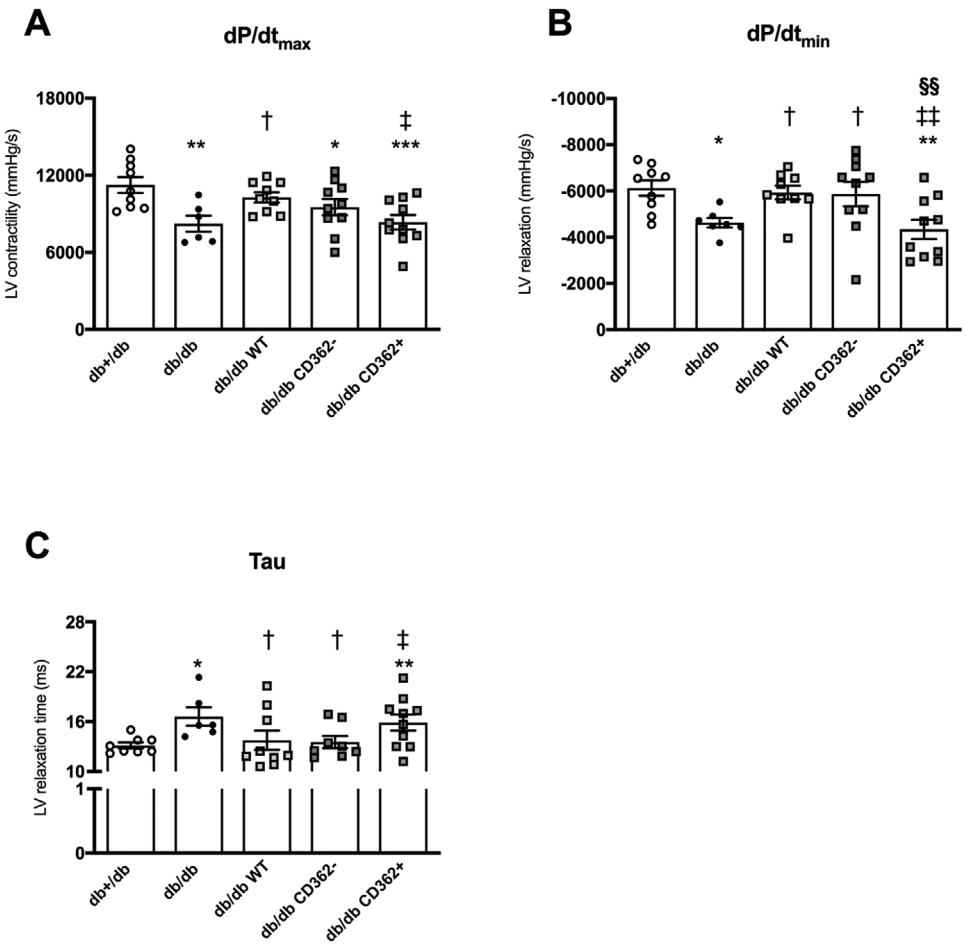

Figure 5. Intravenously applied syndecan-2-selected mesenchymal stromal cells improve myocardial performance in type 2 diabetic db/db mice. Investigation of LV function was performed using the conductance catheter technique. As indices for cardiac contractile function, A) LV contractility (dP/dt_{max} in mmHg s^{-1}), B) LV relaxation (dP/dt_{min} in mmHg s^{-1}), and C) LV relaxation time (Tau in ms) are depicted. Bar graphs represent the mean ± SEM and were analyzed with one-way ANOVA or Kruskal–Wallis test (*$p < 0.05$, **$p < 0.01$, ***$p < 0.001$, ****$p < 0.0001$ vs db+/db; $^{\dagger}p < 0.05$, $^{\dagger\dagger}p < 0.01$, $^{\dagger\dagger\dagger}p < 0.001$, $^{\dagger\dagger\dagger\dagger}p < 0.0001$ versus db/db; $^{\ddagger}p < 0.05$, $^{\ddagger\ddagger}p < 0.01$, $^{\ddagger\ddagger\ddagger}p < 0.001$, $^{\ddagger\ddagger\ddagger\ddagger}p < 0.0001$ vs db/db WT; $^{\S}p < 0.05$, $^{\S\S}p < 0.01$, $^{\S\S\S}p < 0.001$, $^{\S\S\S\S}p < 0.0001$ vs db/db $CD362^{+}$ with $n = 9$ for db+/db, $n = 6$ for db/db, $n = 8$ for db/db WT, $n = 9$ for db/db $CD362^{-}$, and $n = 9$ for db/db $CD362^{+}$ group).

patients who underwent cardiac contractility modulation,[15] in which increased intensity distribution of titin was observed and further associated with improved LV function in both these studies.

The difference between titin isoforms N2B and N2BA cannot be distinguished via MALDI-IMS. Distinction between the isoforms can, however, be made by ion mobility, which detects unique peptide sequences. However, these unique peptide sequences are significantly underrepresented compared to other peptides after tryptic digestion and pose a challenge for isoform identification. Under normal conditions, the N2BA isoform is expressed at lower levels compared to N2B. A shift in the titin isoform profile or general titin hypophosphorylation results in the development of cardiac dysfunction.[7,17] In the present study, significantly lower titin intensity distribution was detected in db/db mice compared to db+/db mice using MALDI-IMS. Further evaluation of protein levels indicated a lower N2BA/N2B ratio and titin hypophosphorylation in db/db versus db+/db mice. In accordance to the literature, where diabetes mellitus is associated with low PKG and PKA activity[5,25] leading to titin hypophosphorylation and cardiomyocyte stiffness,[26,27] we observed a reduction in LV PKG and PKA activity in db/db compared to db+/db animals. With respect to MSC application, MALDI-IMS revealed higher intensity distribution of cardiac titin in db/db mice treated with $CD362^{+}$ MSC, which was accompanied by a shift in the N2BA/N2B ratio toward the more compliant N2BA isoform. In contrast, WT and $CD362^{-}$ MSC administration in db/db mice had no effect on titin intensity distribution or the N2BA/N2B ratio. Surprisingly, we detected no improvement of diastolic performance in db/db $CD362^{+}$ mice, whereas db/db WT and db/db $CD362^{-}$ animals displayed improved diastolic LV function. This may be due to the low PKG and PKA activity, and therefore titin hypophosphorylation in db/db $CD362^{+}$ treated mice. In contrast, concomitant with the increase in titin phosphorylation, application of WT and $CD362^{-}$ MSC normalized PKG activity to control levels. These data indicate that treatment of db/db mice with WT or $CD362^{-}$ MSC can normalize titin phosphorylation and PKG activity, and that this normalization of PKG activity likely

underlies the restoration of cardiac diastolic performance in these animals.

Since PKG is a downstream target of nitric oxide (NO) and an impaired NO bioavailability, hallmark of endothelial dysfunction,[28] is known to decrease cardiomyocyte PKG activity, leading to cardiomyocyte and diastolic stiffness,[5,27,29] the WT and CD362$^-$ MSC-mediated increase in PKG activity is suggested to be due to an improvement in endothelial function in the db/db mice. This hypothesis is supported by our own previous findings illustrating that MSC increase the NO bioavailability in endothelial cells under hyperglycemic conditions.[5] This MSC-mediated improvement in NO bioavailability was associated with an increase in vascularization in diabetic mice.[5] Based on the finding of De Rossi and colleagues,[30] who demonstrated that released syndecan-2/CD362 induces anti-angiogenic effects, we suggest that CD362$^+$ MSC have less pronounced pro-angiogenic/endothelial-protective effects compared to WT and CD362$^-$ MSC. Consequently, the lack of improvement in diastolic performance following CD362$^+$ MSC application in db/db mice could be explained by the low PKG activity and subsequent titin hypophosphorylation in db/db CD362$^+$ mice.

4. Summary and Conclusion

The present study evaluated LV tissue sections via MALDI-IMS, from control db+/db, diabetic db/db mice, and db/db mice who received therapeutic MSCs. Subsequent bottom-up LC-MS was used to identify spatial protein signatures and to assess the therapeutic response to syndecan-2/CD362$^+$-selected MSC. The LV architecture is composed of differently orientated fibers, building the endo-, meso-, and epicardium;[11,31] extraction of these specific regions via tissue microdissection is still challenging. The process is labor intensive and yields little knowledge about the actual spatial distribution of pathophysiological regions.[10] The specimen-based proteomic approach, which was used in the present study, revealed overall alterations in intensity distribution of proteins belonging to cardiac energy metabolism and contractile apparatus in diabetic db/db mice. Specifically, cardiac myosin-6/7 and titin intensity distributions were reduced in db/db compared to db+/db mice, but were normalized by treatment with CD362$^+$ MSC, whereas WT and CD362$^-$ MSC had no effect on titin and cardiac myosin-6/7 intensity distribution. Subsequent analyses of titin phosphorylation and PKG activity indicated that WT and CD362$^-$ MSC ameliorated titin hypophosphorylation, leading to improved diastolic performance in db/db mice. In contrast, CD362$^+$ MSC did not improve titin phosphorylation, resulting in no improvement of diastolic performance.

Thus, we confirm that IMS is able to assess differences in titin intensity distribution following MSC application, already at the early onset of experimental diabetic cardiomyopathy. However, to assess the therapeutic efficacy of MSC treatment, in terms of detecting molecular changes underlying the MSC-mediated improvement in diastolic performance, analysis of titin phosphorylation is required.

5. Experimental Section

Mesenchymal Stromal Cell Preparation: Bone marrow-derived WT-MSC (WT), CD362$^-$ MSC (CD362$^-$), and CD362$^+$ MSC (CD362$^+$) from the same donor were provided by Orbsen Therapeutics Ltd. (Galway, Ireland).[18] Informed consent was obtained for all bone marrow samples according to the Ethics Ref. C.A.02/08. In brief, mononuclear cells (MNCs) were isolated by Ficoll density gradient centrifugation (GE Health Care Bio-Sciences, Buckinghamshire, UK) and ACK Lysis Buffer (Life Technologies, California, USA) employed for erythrocyte lysis. MNCs were then analyzed for expression of CD235-eFluor 450 (clone 6A7M, dilution 1:1000, eBioscience, Hatfield, UK), CD45-FITC (clone HI30, dilution 1:25, BD Biosciences, Oxford, UK), CD271-PE (clone ME20.4-1.H4, dilution 1:50, Miltenyi Biotec, Bergisch Gladbach, Germany), and CD362-APC (clone 305515, dilution 1:50, R&D Systems, Abingdon, UK). The viability dye Sytox Blue (Life Technologies, California, USA) was used to exclude dead cells. Using appropriate controls including fluorescence minus one, gates were assigned and the CD362$^+$CD271$^+$ population (Figure S1, Supporting Information) was sorted using a BD FACS Aria (BD Biosciences, Oxford UK). The mean number of CD362$^+$CD271$^+$ cells isolated form the donors used in this study was 5419 ± 2359 (n = 3). Cells were plated, expanded in culture, and cryopreserved at p2 for shipment to consortia partners. To obtain data for post-sort analysis a minimum of 0.5–1 × 10^6 events were acquired at the time of sorting. Post-sort purities were routinely ≥98% with ≥90% viability. Data were analyzed using FlowJo software (Tree Star, Inc., Ashland, OR, USA).

Experimental Model: Heterozygous (db+/db) and homozygous (db/db) BKS.Cg-m+/+Lepr^{db}/BomTac mice (Taconic, Skensved, Denmark), carrying a leptin receptor mutation, were used as a model for human type 2 diabetes mellitus. At the age of 20 weeks, mice were intravenously injected with 200 µL PBS containing either 1 × 10^6 WT, CD362$^-$, or CD362$^+$ MSC. Animals treated with the same volume of PBS served as controls. Four weeks later, mice were hemodynamically characterized, sacrificed, and the LV was excised for further analysis. All experimental procedures were performed according to European legislation (Directive 2010/63/EU) and approved by the local animal welfare committee (Landesamt für Gesundheit und Soziales, Berlin, Germany, G0254/13).

Tissue Preparation: After hemodynamic measurement, LV were harvested, immediately snap frozen in liquid nitrogen, and stored at −80 °C until further processing. In addition to the frozen samples, one part of the LV was stored in formalin for paraffin embedding.

Cardiac Proteome Analysis by MALDI-Imaging Mass Spectrometry: As described previously,[12,13] MALDI-IMS was performed to determine region-dependent protein expression on LV sections. In brief, LV samples were fixed with paraformaldehyde, washed and embedded in paraffin. Afterward, tissue sections of 7 µm were transferred onto indium–tin-oxide slides (Bruker Daltonik, Bermen, Germany). Subsequently, sections were dewaxed and passed through decreasing concentrations of ethanol.[32] Antigen retrieval was performed according to Gustafsson and colleagues.[33] Next, 200 µL of a trypsin solution (20 µg) containing 20 mM ammonium bicarbonate/acetonitrile (ratio 9:1) was applied via an automated spraying device (ImagePrep; Bruker Daltonik) directly onto the sections.[32] Finally, matrix solution was applied in the same way. Data acquisition was performed on an Autoflex III MALDI-TOF/MS in a raster width of 80 µm by using the flexControl 3.0 and flexImaging 3.0 software (Bruker Daltonik).

In order to identify the proteins corresponding to the detected discriminative m/z values, adjacent tissue sections were analyzed via the "bottom-up"—nano liquid chromatography (Dionex Ultimate 3000, Thermo Fischer)—MS/MS (ESI-QTOF; Bruker Daltonik) approach.[13] To perform an "on tissue digestion "(surface), trypsin solution was applied via ImagePrep and incubated for 3 h at 37 °C. Peptides for following nUPLC-MS/MS analysis were extracted directly from adjacent tissue sections into 40 µL of 0.1% trifluoroacetic acid and incubated for 15 min at room temperature.

The respective mass spectra were analyzed with the *Mus musculus* protein database from UniProt database and a LC-MS/MS reference list. Therefore, the following parameters were set: i) taxonomy: *M. musculus*, ii) proteolytic enzyme: trypsin, iii) peptide tolerance: 10 ppm, iv) maximum of accepted missed cleavages: 1, v) peptide charge: 2+, 3+, 4+, vi) variable modification: oxidation (M), vii) MS/MS tolerance: 0.05Da, and viii)

MOWSE score > 25. The comparison of MALDI-imaging and LC–MS/MS m/z values required the identification of more than one peptide (mass differences <0.9 Da).[34]

Analysis of Cardiac All-Titin Phosphorylation: As described in detail elsewhere,[5,17] frozen LV samples were solubilized and heated, followed by gel electrophoresis. To determine content of the N2BA and N2B isoform, gels were stained overnight with SYPRO Ruby (Thermo Fisher Scientific). With respect to isoform phosphorylation, a Pro-Q Diamond phosphoprotein staining was performed. After the corresponding staining, gels were subsequently analyzed on the LAS-4000 Image Reader (460 nm/605 nm Ex/Em; 2s illumination) using the Multi Gauge V3.2 and AIDA software. Total titin isoform composition (N2BA + N2B) and phosphorylation were assumed to be 100% and expressed as relative values in percentage.

Determination of Myocardial Protein Kinase G Activity: Analogous to the analysis of cardiac titin, LV tissue was first homogenized and centrifuged. As previously described,[5] resulting supernatants were incubated with a solution allowing incorporation of ^{32}P into a substrate depending on myocardial protein kinase G activity.[26] PKG activity was expressed as percentage of the control group, set as 100%.

Determination of Myocardial Protein Kinase A Activity: To determine myocardial PKA activity, a nonradioactive PKA kinase activity assay (Enzo Life Science, Farmingdale, NY, USA) was performed.[5] According the manufacturers protocol, supernatants were added to the substrate plate after sample homogenization. Addition of ATP initiated the kinase reaction and intensity of color development was measured at 450 nm. Analogous to PKG, activity was expressed as percentage of the control group, set as 100%.

Hemodynamic Measurements: To assess LV systolic and diastolic function, hemodynamic measurements via conductance catheter technique were performed. Four weeks after cell or PBS application, mice were first anesthetized (0.8–1.2 g kg^{-1} urethane i.p. and 0.05 mg kg^{-1} buprenorphine i.p.) and artificially ventilated. Afterward, a 1.2 F conductance catheter (Scisense Inc., Ontario, Canada) was positioned into the LV to record LV contractility (dP/dt_{max}), LV relaxation (dP/dt_{min}) and LV relaxation time (Tau).[35]

Statistical Analysis: All data were expressed as mean ± SEM and statistical analysis was performed using the GraphPad Prism 8 Software (GraphPad Software, La Jolla, USA). Differences were considered significant at $p < 0.05$ using one-way ANOVA with LSD post hoc test (parametric data) or Kruskal–Wallis test with Dunn´s post hoc test (non-parametric data).

With respect to MALDI-IMS approach, data were analyzed using the SCiLS Lab software (Version 2020a, SCiLS GmbH, Bremen, Germany).[13] MALDI-IMS raw data were first imported into the SCiLS Lab software and converted to the SCiLS SL file format. The import settings in SCiLS Lab were as follows: no baseline removal and total ion count preserving. Peak finding and alignment were accomplished using a standard segmentation pipeline.[36] In order to minimize the uncertainty interval to inter-spectra alignment problems, the SCilS interval-processing mode "maximal value on interval" was used. The following settings were used: interval width 0.337 Da; interval processing, mean; smoothing strength, medium; and Sigma, 1×10^6. PCA was further used to determine the largest difference between the groups. The settings for PCA were as follows: denoising, weak; interval width, 0.337 Da; interval processing, maximum number of components, five; scaling, unit variance; and spectrum mode, "individual". In order to determine discriminative and characteristic m/z values (peptides) in the LV tissue specimens of the different groups, a receiver operating characteristic (ROC) analysis was performed. Since the number of spectra from each group should be approximately the same, 1700 randomly selected spectra per group were used for the pairwise comparison. The area under the ROC curve (AUC) varies between 0 and 1, where values of ≈0 and 1 indicate a discriminating property, and values of ≈0.5 indicate a non-discriminating property. For those peaks with a ROC score of the AUC >0.6 or <0.4, a univariate hypothesis test (Wilcoxon rank sum test) was used to ensure the statistical significance ($p \leq 0.01$).

Supporting Information

Supporting Information is available from the Wiley Online Library or from the author.

Acknowledgements

This study was supported by the European 7th Framework Consortium Repair of Diabetic Damage by Stromal Cell Administration (REDDSTAR; Grant: HEALTH.2012.2.4.3-1) to S.E., C.T., S.V.L. and T.O.B. The authors further acknowledge support from the German Research Foundation (DFG) and the Open Access Publication Funds of the Charité – Universitätsmedizin Berlin. The authors would like to acknowledge Angelika Krajewski and Gwendolin Matz for excellent technical support. Furthermore, the authors would like to thank Nicola Brindle for scientific language check and editing.

Open access funding enabled and organized by Projekt DEAL.

Correction added on January 18, 2021, after first online publication: Dr. Kathleen Pappritz was designated as corresponding author.

Conflict of Interest

Dr. Elliman is the Chief Scientific Officer and Dr. O'Flynn is the Head of Process Development at Orbsen Therapeutics Ltd. (Galway, Ireland), a company that is developing the $CD362^+$ MSC for therapeutic purposes. The other authors declare no conflict of interest.

Data Availability Statement

All datasets used and/or analyzed during the current study are available from the corresponding author on reasonable request.

Keywords

diabetic cardiomyopathy, matrix-assisted laser desorption/ionization imaging mass spectrometry, syndecan-2/$CD362^+$-selected stromal cells, titin

Received: June 9, 2020
Revised: October 12, 2020
Published online: December 10, 2020

[1] J. A. Beckman, M. A. Creager, P. Libby, *JAMA, J. Am. Med. Assoc.* **2002**, *287*, 2570.
[2] S. Rubler, J. Dlugash, Y. Z. Yuceoglu, T. Kumral, A. W. Branwood, A. Grishman, *Am. J. Cardiol.* **1972**, *30*, 595.
[3] S. Van Linthout, F. Spillmann, A. Riad, C. Trimpert, J. Lievens, M. Meloni, F. Escher, E. Filenberg, O. Demir, J. Li, M. Shakibaei, I. Schimke, A. Staudt, S. B. Felix, H. P. Schultheiss, B. De Geest, C. Tschope, *Circulation* **2008**, *117*, 1563.
[4] C. Tschope, T. Walther, J. Koniger, F. Spillmann, D. Westermann, F. Escher, M. Pauschinger, J. B. Pesquero, M. Bader, H. P. Schultheiss, M. Noutsias, *FASEB J.* **2004**, *18*, 828.
[5] S. Van Linthout, N. Hamdani, K. Miteva, A. Koschel, I. Muller, L. Pinzur, Z. Aberman, K. Pappritz, W. A. Linke, C. Tschope, *Stem Cells Transl. Med.* **2017**, *6*, 2135.
[6] C. Tschope, S. Van Linthout, *Curr. Heart Failure Rep.* **2014**, *11*, 436.
[7] N. Hamdani, W. J. Paulus, *Circulation* **2013**, *128*, 5.
[8] S. Cosson, J. P. Kevorkian, *Diabetes Metab.* **2003**, *29*, 455.
[9] a) S. Meding, A. Walch, in *Cell Imaging Techniques: Methods and Protocols*, (Eds: D. J. Taatjes, J. Roth), Humana Press, Totowa, NJ **2013**, 537; b) B. D. Leinweber, G. Tsaprailis, T. J. Monks, S. S. Lau, *J. Am. Soc. Mass Spectrom.* **2009**, *20*, 89.

[10] A. Walch, S. Rauser, S. O. Deininger, H. Hofler, *Histochem. Cell Biol.* **2008**, *130*, 421.
[11] K. Pappritz, J. Grune, O. Klein, N. Hegemann, F. Dong, M. El-Shafeey, J. Lin, W. M. Kuebler, U. Kintscher, C. Tschope, S. Van Linthout, *Sci. Rep.* **2020**, *10*, 3629.
[12] O. Klein, K. Strohschein, G. Nebrich, J. Oetjen, D. Trede, H. Thiele, T. Alexandrov, P. Giavalisco, G. N. Duda, P. von Roth, S. Geissler, J. Klose, T. Winkler, *Proteomics* **2014**, *14*, 2249.
[13] O. Klein, T. Hanke, G. Nebrich, J. Yan, B. Schubert, P. Giavalisco, F. Noack, H. Thiele, S. A. Mohamed, *Proteomics - Clin. Appl.* **2018**, *12*, 1700155.
[14] F. Spillmann, S. Van Linthout, G. Schmidt, O. Klein, N. Hamdani, T. Mairinger, F. Krackhardt, B. Maroski, T. Schlabs, S. Soltani, S. Anker, E. V. Potapov, D. Burkhoff, B. Pieske, C. Tschope, *Eur. Heart J.* **2019**, *40*, 2164.
[15] C. Tschope, S. Van Linthout, F. Spillmann, O. Klein, S. Biewener, A. Remppis, D. Gutterman, W. A. Linke, B. Pieske, N. Hamdani, M. Roser, *Int. J. Cardiol.* **2016**, *203*, 1061.
[16] M. T. Waddingham, A. J. Edgley, H. Tsuchimochi, D. J. Kelly, M. Shirai, J. T. Pearson, *World J. Diabetes* **2015**, *6*, 943.
[17] N. Hamdani, C. Franssen, A. Lourenco, I. Falcao-Pires, D. Fontoura, S. Leite, L. Plettig, B. Lopez, C. A. Ottenheijm, P. M. Becher, A. Gonzalez, C. Tschope, J. Diez, W. A. Linke, A. F. Leite-Moreira, W. J. Paulus, *Circ.: Heart Failure* **2013**, *6*, 1239.
[18] C. Masterson, J. Devaney, S. Horie, L. O'Flynn, L. Deedigan, S. Elliman, F. Barry, T. O'Brien, D. O'Toole, J. G. Laffey, *Anesthesiology* **2018**, *129*, 502.
[19] L. A. McDonnell, A. Rompp, B. Balluff, R. M. Heeren, J. P. Albar, P. E. Andren, G. L. Corthals, A. Walch, M. Stoeckli, *Anal. Bioanal. Chem.* **2015**, *407*, 2035.
[20] a) Á. Kovács, A. Alogna, H. Post, N. Hamdani, *Neth. Heart J.* **2016**, *24*, 268; b) N. Hamdani, M. de Waard, A. E. Messer, N. M. Boontje, V. Kooij, S. van Dijk, A. Versteilen, R. Lamberts, D. Merkus, C. Dos Remedios, D. J. Duncker, A. Borbely, Z. Papp, W. Paulus, G. J. Stienen, S. B. Marston, J. van der Velden, *J. Muscle Res. Cell Motil.* **2008**, *29*, 189.
[21] D. Cruz-Topete, E. O. List, S. Okada, B. Kelder, J. J. Kopchick, *J. Proteomics* **2011**, *74*, 716.
[22] M. F. Essop, W. A. Chan, S. Hattingh, *Cardiovasc. J. Afr.* **2011**, *22*, 175.
[23] S. C. Kolwicz, Jr., S. Purohit, R. Tian, *Circ. Res.* **2013**, *113*, 603.
[24] a) V. A. Gault, B. D. Kerr, P. Harriott, P. R. Flatt, *Clin. Sci.* **2011**, *121*, 107; b) S. Yoshida, H. Tanaka, H. Oshima, T. Yamazaki, Y. Yonetoku, T. Ohishi, T. Matsui, M. Shibasaki, *Biochem. Biophys. Res. Commun.* **2010**, *400*, 745.
[25] L. van Heerebeek, N. Hamdani, I. Falcao-Pires, A. F. Leite-Moreira, M. P. Begieneman, J. G. Bronzwaer, J. van der Velden, G. J. Stienen, G. J. Laarman, A. Somsen, F. W. Verheugt, H. W. Niessen, W. J. Paulus, *Circulation* **2012**, *126*, 830.
[26] N. Hamdani, A. S. Hervent, L. Vandekerckhove, V. Matheeussen, M. Demolder, L. Baerts, I. De Meester, W. A. Linke, W. J. Paulus, G. W. De Keulenaer, *Cardiovasc. Res.* **2014**, *104*, 423.
[27] W. J. Paulus, C. Tschope, *J. Am. Coll. Cardiol.* **2013**, *62*, 263.
[28] S. Van Linthout, F. Spillmann, M. Lorenz, M. Meloni, F. Jacobs, M. Egorova, V. Stangl, B. De Geest, H. P. Schultheiss, C. Tschope, *Hypertension* **2009**, *53*, 682.
[29] C. Franssen, S. Chen, A. Unger, H. I. Korkmaz, G. W. De Keulenaer, C. Tschope, A. F. Leite-Moreira, R. Musters, H. W. Niessen, W. A. Linke, W. J. Paulus, N. Hamdani, *JACC: Heart Failure* **2016**, *4*, 312.
[30] G. De Rossi, A. R. Evans, E. Kay, A. Woodfin, T. R. McKay, S. Nourshargh, J. R. Whiteford, *J. Cell Sci.* **2014**, *127*, 4788.
[31] R. A. Greenbaum, S. Y. Ho, D. G. Gibson, A. E. Becker, R. H. Anderson, *Heart* **1981**, *45*, 248.
[32] R. Casadonte, R. M. Caprioli, *Nat. Protoc.* **2011**, *6*, 1695.
[33] O. J. Gustafsson, M. T. Briggs, M. R. Condina, L. J. Winderbaum, M. Pelzing, S. R. McColl, A. V. Everest-Dass, N. H. Packer, P. Hoffmann, *Anal. Bioanal. Chem.* **2015**, *407*, 2127.
[34] B. Cillero-Pastor, R. M. Heeren, *J. Proteome Res.* **2014**, *13*, 325.
[35] K. Pappritz, K. Savvatis, K. Miteva, B. Kerim, F. Dong, H. Fechner, I. Muller, C. Brandt, B. Lopez, A. Gonzalez, S. Ravassa, K. Klingel, J. Diez, P. Reinke, H.-D. Volk, S. V. Linthout, C. Tschope, *FASEB J.* **2018**, *32*, 6066.
[36] a) T. Alexandrov, M. Becker, S. O. Deininger, G. Ernst, L. Wehder, M. Grasmair, F. von Eggeling, H. Thiele, P. Maass, *J. Proteome Res.* **2010**, *9*, 6535; b) T. Alexandrov, M. Becker, O. Guntinas-Lichius, G. Ernst, F. von Eggeling, *J. Cancer Res. Clin. Oncol.* **2013**, *139*, 85.